Development 129, 347-359 (2002)
Printed in Great Britain © The Company of Biologists Limited 2002
DEV5975

Mutations in *Drosophila myb* lead to centrosome amplification and genomic instability

Siau-Min Fung, Gary Ramsay and Alisa L. Katzen*

Department of Molecular Genetics, University of Illinois at Chicago, College of Medicine, Chicago, IL 60607-7170, USA
*Author for correspondence (e-mail: katzen@uic.edu)

Accepted 22 October 2001

SUMMARY

We have previously established that the single *myb* gene in *Drosophila melanogaster*, *Dm myb*, which is related to the proto-oncogene *Myb*, is required for the G_2/M transition of the cell cycle and for suppression of endoreduplication in pupal wing cells. We now report that studies of the abdominal phenotype in loss-of-function *Dm myb* mutants reveal additional roles for *Dm myb* in the cell cycle, specifically in mitosis. Abdominal epidermal cells that are mutant for *Dm myb* proliferate more slowly than wild-type controls throughout pupation, with particularly sluggish progression through the early stages of mitosis. Abnormal mitoses associated with multiple functional centrosomes, unequal chromosome segregation, formation of micronuclei, and/or failure to complete cell division are common in the later cell cycles of mutant cells. Resulting nuclei are often aneuploid and/or polyploid. Similar defects have also been observed in loss-of-function mutations of the tumor suppressor genes *p53*, *Brca1* and *Brca2*. These data demonstrate that in abdominal epidermal cells, *Dm myb* is required to sustain the appropriate rate of proliferation, to suppress formation of supernumerary centrosomes, and to maintain genomic integrity.

Key words: *Drosophila*, *myb*, Transcription factor, Mitosis, Centrosomes, Genomic instability

INTRODUCTION

Failure to precisely regulate chromosome duplication and segregation leads to genomic instability, a term encompassing an assortment of genomic alterations including loss or gain of entire chromosomes, and other chromosomal abnormalities, such as rearrangements, translocations, amplifications and deletions. Genomic instability can result in cell or organismal death (Chester et al., 1998; Gao et al., 2000; Reed, 1999), is associated with premature aging disorders (Karow et al., 2000), and is considered to be a primary driving force of multistep carcinogenesis (Nowell, 1976; Solomon et al., 1991).

Genomic integrity is maintained by cell cycle checkpoints that monitor DNA replication and detect cellular/DNA damage (Hartwell et al., 1994). Centrosomes organize the poles of the mitotic bipolar spindle and play a key role in genomic stability by ensuring balanced chromosome segregation (Sluder and Hinchcliffe, 1999). When a mitotic cell contains more than two functional centrosomes, a multipolar spindle can be formed that either randomly distributes chromosomes into multiple daughter cells or results in failure to complete cell division (Fukasawa et al., 1996; Sluder and Hinchcliffe, 1999). Either way, the consequence is genomic instability, a hallmark of many aggressive tumors (Pihan et al., 1998; Salisbury et al., 1999). Abnormally high numbers of centrosomes have been detected in many human tumor cells, an anomaly ascribed to their lack of the tumor suppressor proteins p53 (TP53 – Human Gene Nomenclature Database), BRCA1 or BRCA2 (Fukasawa et al., 1996; Tutt et al., 1999; Xu et al., 1999).

The vertebrate Myb gene family consists of three closely related members, *Myb* (c-*myb*), *Mybl1* (A-*myb*) and *Mybl2* (B-*myb*). Myb genes encode DNA-binding proteins that regulate transcription and have been implicated in regulatory decisions affecting cell proliferation, differentiation and apoptosis (Oh and Reddy, 1999; Weston, 1998). Mutant versions of *Myb* have been implicated in the genesis of neoplastic disease in chickens, mice and humans (Oh and Reddy, 1999). *Drosophila melanogaster* possesses a single *myb* gene (*Dm myb*; *Myb* – FlyBase), which contains four regions of homology with the vertebrate Myb genes (Bishop et al., 1991; Katzen et al., 1985; Peters et al., 1987). The *Dm myb* gene product, DMyb (Myb – FlyBase), shares several biochemical properties with the vertebrate family of Myb proteins, including binding to a similar consensus sequence and the ability to activate transcription from a reporter construct regulated by vertebrate Myb proteins (Jackson et al., 2001).

We have previously reported the isolation of temperature-sensitive, recessive lethal mutations in *Dm myb*. Mutant phenotypes revealed a requirement for *Dm myb* in diverse cellular lineages throughout development (Katzen and Bishop, 1996). Even when mutants are raised at temperatures permissive for viability, adults display abnormalities, including cuticular defects in wings and abdomens. Analysis of the wing phenotype demonstrated that *Dm myb* is required for both

promotion of the G_2/M transition and suppression of endoreduplication in pupal wing cells (Katzen et al., 1998).

The abdominal phenotype in *Dm myb* mutants, which includes missing bristles and patches of undifferentiated and unpigmented cuticle, is also suggestive of a proliferation defect. However, there are notable differences between wing and abdominal phenotypes (see Results), which may reflect the fact that the post-embryonic program for the development of abdominal epidermis is distinct from that of the rest of the adult epidermis (Cohen, 1993; Fristrom and Fristrom, 1993). The epidermis of the thorax (including the wing) and head is formed from imaginal discs, which contain diploid cells that proliferate throughout larval development, completing only their final one or two cell divisions during early pupation. By contrast, the abdominal epidermis is formed from small nests of imaginal cells, called abdominal histoblasts, which do not divide during larval development, but undergo rapid proliferation after puparium formation (Madhavan and Madhavan, 1980).

The differences in *Dm myb* mutant phenotype between wings and abdomens at the cuticular level, together with the divergences in developmental programs, suggested that an analysis of the cellular basis of the abdominal phenotype might reveal more about *Dm myb* function. We now report distinct differences between the cellular defects in mutant *Dm myb* wing and abdominal cells, and we provide evidence that in proliferating abdominal epidermal cells, *Dm myb* is required to sustain the appropriate rate of proliferation, to suppress formation of supernumerary centrosomes and to maintain genomic integrity.

MATERIALS AND METHODS

Drosophila stocks

Generation of mutant *Dm myb* alleles, myb^1 and myb^2, on a *white* chromosome; construction of lines carrying a wild-type *Dm myb* rescue transgene, P(w^+,myb^+); and the Df(1)sd^{72b26} chromosome, which deletes a region including *Dm myb*, have been described previously (Katzen and Bishop, 1996). Dp(1:Y)$shi^+Y^{\#3}$ is a specialized Y chromosome that carries a region of the X chromosome, including *Dm myb* (13F1-4 to 14F4-6) (Poodry, 1980). The only apparent difference between Df(1)sd^{72a} and Df(1)sd^{72b26} (13F1-14B1) (Craymer and Roy, 1980) chromosomes is that the latter carries a recessive lethal mutation which is not closely linked with the deleted region (A. L. K., unpublished). Therefore, Df(1)sd^{72a}, but not Df(1)sd^{72b26}, is rescued by the Dp(1:Y)$shi^+Y^{\#3}$ chromosome. Stocks carrying esg^{P3}, esg^{VS8}, Df(2L)TE35D-2 (which deletes *esg*), and hsp70-Gal4 provided by S. Hayashi; UAS-RBF provided by Bruce Edgar; and esg^{k0060}, $RpS3^1$ and $M(3)65F^1$ obtained from Bloomington Stock Center.

Adult abdomen preparation

Matings were performed at 18°C, and female white prepupae were collected and shifted to indicated temperatures. For mutants shifted to non-permissive temperatures, pharate adults were dissected out of pupal cases. Viable and pharate adults were preserved in 100% isopropanol. Abdomens were dissected and immersed in mineral oil for imaging using a Kodak Science Digital MDS 120 camera and a dissecting microscope.

Preparation and fluorescent staining of the abdominal epidermis from larvae and pupae

The enhancer trap insert esg^{P3}, which expresses β-galactosidase in larval abdominal histoblasts (Hayashi et al., 1993) was used to identify these cells. Wandering third instar larvae were fixed in 4% paraformaldehyde, 0.1% deoxycholic acid, and 0.1% Tween-20 in phosphate-buffered saline (PBS). Samples were then incubated with mouse anti-β-galactosidase antibodies (Promega, 1:1000), followed by an anti-mouse secondary conjugated to rhodamine (Boehringer Mannheim, 1:10). Finally, samples were stained with DAPI (4′6-diamidine-2-phenylindole) at 0.5 μg/ml, rinsed, and mounted in Vectashield (Vector).

To prepare pupal samples from females of appropriate genotype (see figure legends), control (*w*), myb^1 or myb^2 virgin females were mated with myb^1, myb^2 or Df(1)sd^{72a}/Dp(1:Y)$shi^+Y^{\#3}$ males at 18ºC. Female progeny were selected as larvae and maintained at 18°C until pupariation. White prepupae (0 hours after puparium formation (APF)) were picked and shifted to indicated temperatures for specified times. Pupae were then treated for abdominal epidermal preparation as previously described (Kopp et al., 1997) before fixation. Fixation conditions varied, depending upon the antisera: for PH3 and Bub1 antibodies, 4% paraformaldehyde for 30 minutes at room temperature; and for CP60, CP190 and β-tubulin antibodies, 37% formaldehyde for 5 minutes at room temperature. Immunostaining was performed as previously described (Audibert et al., 1996; Theurkauf, 1994) with the following dilutions for primary antibodies: 1:20 for β-tubulin (Harlan); 1:500 for CP60 and CP190; 1:1000 for Bub1 and PH3 (Upstate Biotech); and 1:10,000 for γ-tubulin (Sigma). Secondary antibodies conjugated to either FITC or rhodamine were purchased from Boehringer Mannheim and used at recommended dilutions. After immunostaining, samples were treated with DAPI at 0.5 μg/ml for 10 minutes, rinsed and mounted. DAPI staining was used to determine and compare the number of abdominal epidermal cells in control and mutant *Dm myb* animals (see Results and Table 1). BrdU labeling was performed as described by Shermoen (Shermoen, 2000), with the only modification being that samples were incubated with BrdU for 1 hour. Samples were imaged either by confocal microscopy (Zeiss LSM 550) or by wide-field microscopy (Zeiss Axioplan2) using a Princeton Instruments Micromax cooled CCD camera.

Fluorescent in-situ hybridization

The probe representing a 359 bp repeat present in X-chromosome heterochromatin was generously provided by Tin Tin Su. Fluorescent in-situ hybridization (FISH) was carried out as described by Dernburg (Dernburg, 2000) with the following modifications: hybridization solution contained 35% formamide, 5× SSC, 100 μg/ml tRNA and 0.1% Tween; probe and chromosomal DNA were denatured for 3 minutes at 92°C; samples were incubated for annealing at room temperature for 3 hours; samples were incubated with PH3 antibodies overnight, after which anti-DIG-rhodamine (Boehringer Mannheim, 1:10) and anti-rabbit-FITC were added together and samples were incubated for 2 hours at room temperature.

Quantitation of DNA content

Abdominal epidermal samples were fixed in 4% paraformaldehyde for 30 minutes and then stained with rhodamine-conjugated phalloidin (Molecular Probes, 5 U/ml) for 30 minutes and DAPI (0.5 μg/ml) for 10 minutes. After mounting in Vectashield, cover slips were sealed and samples were immediately imaged by confocal microscopy (Zeiss LSM 550) under identical conditions, set such that the DAPI fluorescence was within a linear range. Stacks of optical *z*-sections were collected at 2/3 μm intervals. Relative DNA contents of mutant and wild type nuclei were determined using a method similar to those described by others (Euling and Ambros, 1996; Hayashi and Yamaguchi, 1999). Briefly, the public domain NIH Image program 1.61 (http://rsb.info.nih.gov/nih-image/) was used: images were stacked, and the mean fluorescence value of each nucleus for each layer was determined and then multiplied by the area of the nucleus. Total values were obtained for each nucleus by summing the values for each layer. Background levels of signal were measured for all samples. They were low and did not differ significantly between samples.

RESULTS

Abdominal cuticular defects in adult *Dm myb* mutants resemble those observed in *esg* and *cdc2* mutants

In addition to the previously characterized wing phenotype (Katzen et al., 1998), myb^1 and myb^2 mutants raised at temperatures permissive for viability (18°C and 24°C, respectively) also displayed abdominal cuticular defects, including missing and misoriented bristles, and patches of undifferentiated and unpigmented cuticle (Fig. 1B,C,F). The expressivity of the abdominal phenotype varied at viable temperatures, but was stronger and more consistent in pharate adults raised at temperatures restrictive for viability (Fig. 1D,G).

Abdominal and wing phenotypes in *myb* mutants differ in several respects. Mutants wings are the appropriate size, but contain approximately half the number of hairs as wild type. Mutant hairs are considerably larger than normal and often misoriented. Bristles are never missing on mutant wings or elsewhere on the thorax and head, but the mutant bristles are larger and less uniform in orientation (Katzen et al., 1998). By contrast, the remaining abdominal bristles (and hairs) in *Dm myb* mutants appear to be wild type in size, although they are often misoriented (Fig. 1B-D,F,G). Phenotypic distinctions may reflect differences in post-embryonic developmental programs (see Introduction). Indeed, the abdominal phenotype is characteristic of situations in which there are not enough adult epidermal cells to replace all larval cells (Poodry, 1975), and is therefore suggestive of a defect in cell proliferation.

The abdominal phenotype in *Dm myb* mutants resembles those reported for certain mutant alleles of *escargot* (*esg*), which encodes a zinc-finger transcription factor, and for *Drosophila cdc2* (Hayashi et al., 1993; Stern et al., 1993) (Fig. 1H). These defects have been attributed to a failure to suppress endoreduplication in abdominal histoblasts during larval development, thereby producing polyploid abdominal histoblasts that are no longer capable of dividing after puparium formation (Hayashi, 1996; Hayashi et al., 1993). Given the similarity of the phenotypes and our previous finding that when mutant *Dm myb* wing cells were arrested in G_2 of their final cell cycle, they entered into an endoreduplication cycle, it seemed likely that the cellular basis of the *myb* phenotype would be the same as it is in *esg* and *cdc2* mutants. We used the enhancer trap line esg^{P3} (Hayashi et al., 1993) to identify abdominal histoblasts in third instar larvae of wild type, mutant *Dm myb*, and mutant *esg* animals (Fig. 1I-L). As expected, abdominal histoblast nuclei of *esg* mutant larvae were much larger than wild type (Fig. 1L). By contrast, no abnormalities were observed in either the number or appearance of the abdominal histoblasts of mutant *Dm myb* larvae (Fig. 1J,K), indicating that despite similarities in the adult cuticular phenotypes, the cellular basis of these defects in *Dm myb* mutants is different than in *esg* and *cdc2* mutants.

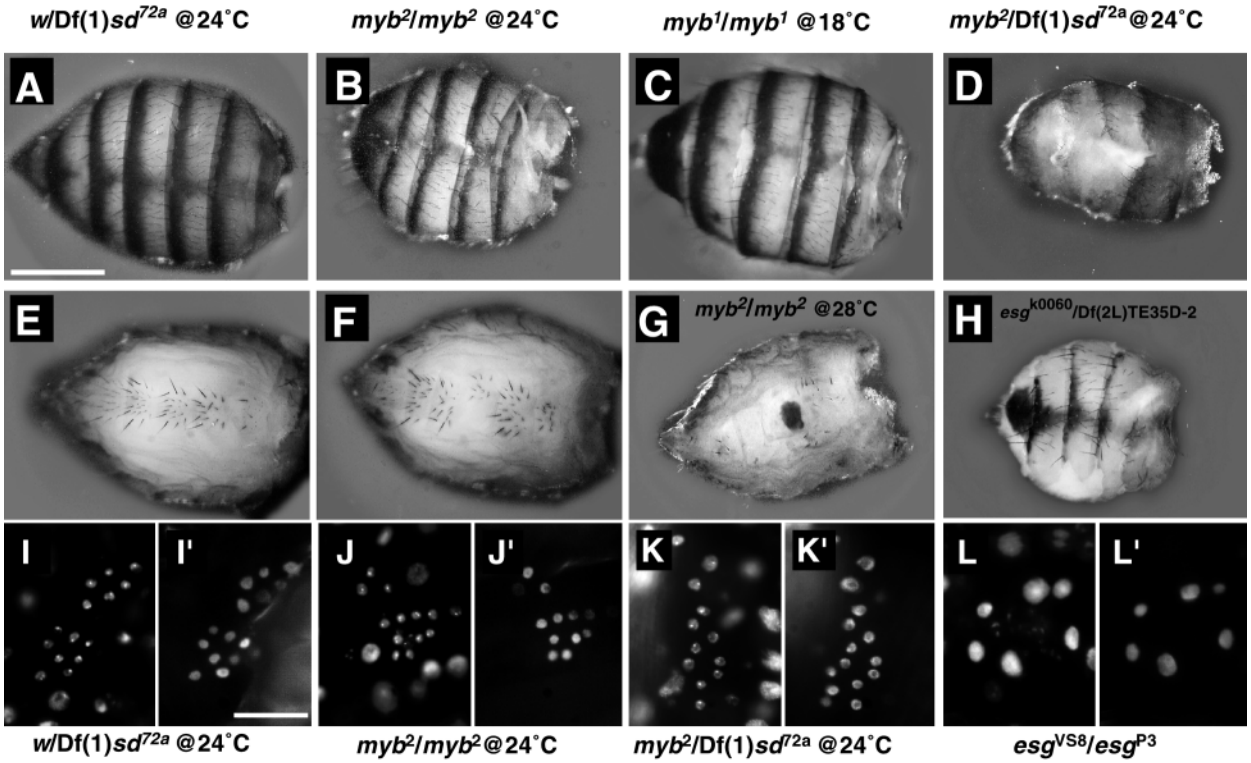

Fig. 1. *Dm myb* mutants have missing and improperly oriented abdominal bristles, and patches of undifferentiated tissue. (A-H) Comparison of wild-type and mutant abdomens. Dorsal (A-D,H) and ventral (E-G) cuticles from female adult abdomens: control *w*/Df(1)sd^{72a} (A,E) flies raised at 24°C; myb^2 (B,F) flies raised at 24°C; (C) myb^1 raised at 18°C; (H) *esg* mutant (esg^{k0060}/Df(2L)TE35D-2) raised at 24°C; pharate adults of myb^2/Df(1)sd^{72a} raised at 24°C (D); and pharate adults of myb^2 raised at 28°C (G). (I-L) Comparison of wild-type and mutant abdominal histoblast nuclei in third instar larvae raised at 24°C. All nuclei within the field were visualized by DAPI staining. (I′-L′) Abdominal histoblast nest cells were identified by using β-galactosidase antibodies and the enhancer trap insert esg^{P3}. (I) Control *w*; esg^{P3}/+; (J) myb^2; esg^{P3}/+; (K) myb^2/Df(1)sd^{72a}; esg^{P3}/+; (L) esg^{VS8}/esg^{P3}. Scale bars: in A, 0.5 mm for A-H; in I′, 0.05 mm in I-L′.

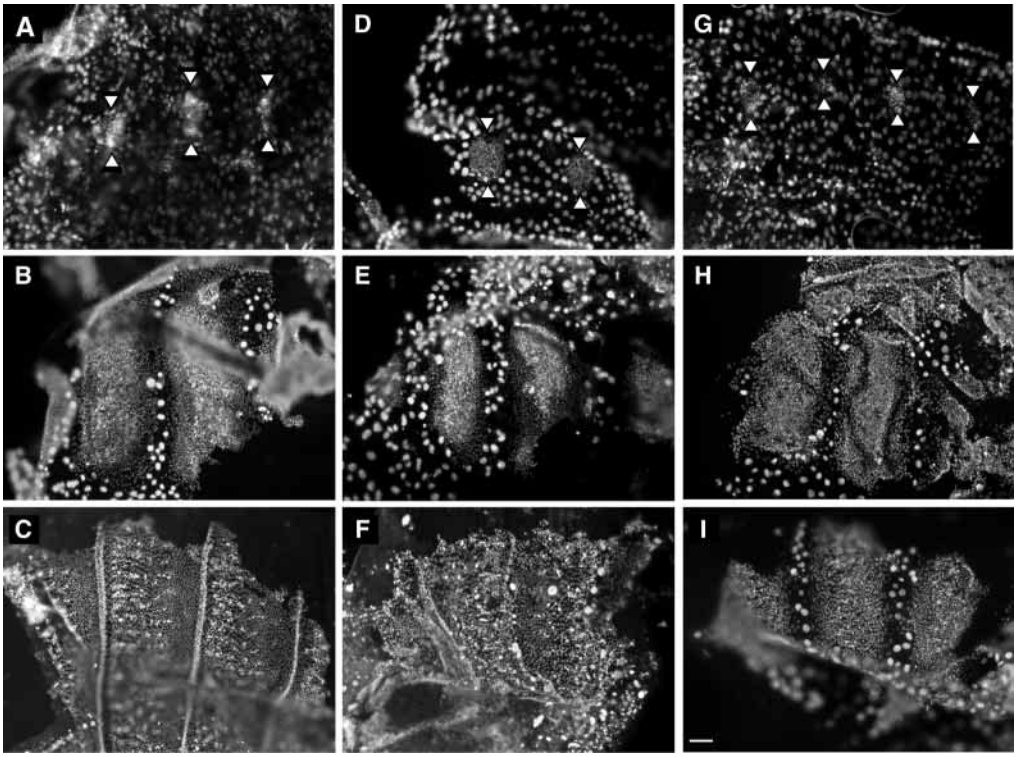

Fig. 2. Abdominal development is delayed in *Dm myb* mutants. At specified timepoints (hours after puparium formation), the abdominal epidermis was dissected from females that had been raised at 18°C until puparium formation and then shifted to 24°C for continued development. Samples were stained with DAPI to visualize nuclei. Large nuclei represent larval polyploid cells; small nuclei correspond to the diploid nuclei of abdominal histoblast cells. (A-C) *w*/Df(1)*sd*^{72a} controls at 13 (A), 30 (B), and 42 (C) hours APF; (D-F) *myb*^{2} at 18 (D), 42 (E) and 51 (F) hours APF; (G) *myb*^{2}/Df(1)*sd*^{72a} at 42 hours APF; (H) *myb*^{2}/Df(1)*sd*^{72a}; P(*w*$^{+}$, *myb*$^{+}$) at 30 hours APF; and (I) *myb*^{1} at 36 hours APF. Arrowheads indicate small histoblast nests. Scale bar: 0.05 mm.

Abdominal histoblasts that are mutant for *Dm myb* proliferate more slowly than wild-type cells

As no defects were apparent in the larval abdominal histoblasts of *Dm myb* mutants, we examined their proliferation during pupal development. Female animals were staged as white prepupae and incubated at 24°C (unless otherwise indicated) for specified time periods. Wild-type controls carried the parental *white* (*w*) chromosome from which the *Dm myb* mutants were generated, over a deficiency chromosome (Df(1)*sd*^{72a}) that deletes the *Dm myb* gene. The deficiency chromosome was used experimentally to reduce the *Dm myb* activity of the hypomorphic alleles. No significant differences were observed between *w* homozygotes and *w*/Df(1)*sd*^{72a} females (not shown).

Several types of defects were observed in this analysis. When abdominal epidermal cells were treated with the DNA stain DAPI, it was apparent that abdominal epidermal development was considerably slower in *Dm myb* mutants than in wild-type controls (Fig. 2). For example, *myb*^{2} abdomens were less developed at 42 hours APF than were control abdomens at 30 hours APF (Fig. 2B,E). When compared with controls at 18 and 24 hour APF, there were approximately half the number of histoblast nuclei in *myb*^{2} mutants, indicating that mutant cells were about one cell division cycle behind. The delay was more pronounced when *Dm myb* activity was further reduced by either carrying *myb*^{2} over Df(1)*sd*^{72a} (non-permissive for viability at 24°C; Fig. 2G) or by shifting *myb*^{2} homozygotes to 28°C (not shown). At 18 and 24 hours APF, *myb*^{2}/Df(1)*sd*^{72a} animals had an average of one-sixth (ranging from one-eighth to a quarter) the number of abdominal histoblasts as controls, suggesting a lag of about two to three cell cycles. Double staining with DAPI and rhodamine-labeled phalloidin (an F-actin specific stain that highlights cell boundaries) showed that at these time points, each cell contained a single nucleus (not shown).

The spreading of histoblast cells to displace adjacent larval epidermal cells, and the subsequent flattening of the adult cells, also occurred more slowly in *Dm myb* mutants. The rate of abdominal development was returned to normal when a wild-type *Dm myb* transgene was reintroduced into *myb*^{2}/Df(1)*sd*^{72a} animals (Fig. 2H), demonstrating that the defects in abdominal development were specifically due to reductions in *Dm myb* function. There was no evidence of elevated apoptosis in *Dm myb* mutants, either by DAPI staining (pyknotic nuclei) or by TUNEL assay (not shown). Therefore, we conclude that the differences in developmental rates can largely be accounted for by differing rates of cell proliferation and spreading, rather than cell death.

In previous studies, the *myb*^{1} allele displayed a stronger phenotype than *myb*^{2} when the flies were raised at the same temperature (Katzen and Bishop, 1996; Katzen et al., 1998). This is not the case, however, in abdominal development. At 24°C, the rate of abdominal histoblast proliferation and spreading for *myb*^{1} was somewhat faster than for *myb*^{2} (Fig. 2I), and the mitotic defects were similar for both alleles. At 18°C, the rate of abdominal development appeared to be nearly normal in both *myb*^{1} and *myb*^{2} mutants (not shown). As the *myb*^{1} allele is less healthy and more difficult to work with at 24°C than *myb*^{2}, we concentrated on the latter for these studies, although similar results were obtained with both mutants.

Delayed and abnormal mitoses occur in abdominal epidermal cells of *Dm myb* mutants

We used an antibody for a mitotic-specific phospho-epitope on histone H3 (PH3) (Hendzel et al., 1997) to identify mitotic abdominal histoblasts. To compare mutant and wild-type cells at the same time points during pupal development, abdominal epidermal samples were prepared from controls and *Dm myb* mutants at 24 hours APF. To compare mutant and wild type

Table 1. Mitotic index and distribution of mitotic stages in wild-type and and *Dm myb* mutants

Hours APF	Total number of cells (number of abdomens)	Mitotic index (% of PH3 staining cells)	% of PH3 staining cells		% of PH3 staining cells in specific mitotic stages		
			Pre-prophase*	Prophase†	Pre-prophase and prophase combined	Prometaphase metaphase	Anaphase and early telophase
w/Df(1)sd72a							
24 hours APF	6 491 (3)	2.7%±0.4§	1.1%	10.8%	11.9%	51.1%	37.0%
30 hours APF	9 006 (2)	3.2%±0.04	0.3%	18.7%	19.0%	45.1%	35.9%
w, myb²/w, myb²							
24 hours	2 523 (4)	3.5%±0.6	0%	19.1%	19.1%	56.2%	24.8%
40-42 hours	6 489 (4)	1.9%±0.5	13.6%	20.8%	34.4%	48.0%	17.6%
44-46 hours	9 468 (4)	2.3%±0.3	20.6%	14.0%	34.6%	45.8%	19.6%
48-50 hours	11 321 (4)	1.1%±0.1	31.1%	11.5%	42.6%	36.9%	20.5%
w, myb²/Df(1)sd^72a							
24 hours	662 (5)	5.7%±0.7	7.9%	34.2%	42.1%	42.1%	15.8%
40-42 hours	2 501 (7)	4.2%±1.6	20.0%	24.8%	44.8%	35.2%	20.0%
44-46 hours	4 410 (7)	4.2%±1.4	41.9%	9.2%	51.1%	37.1%	11.8%
48-50 hours	2 753 (4)	3.8%±1.1	44.2%	11.6%	55.8%	19.2%	25.0%

*'Pre-prophase' cells are defined here as cells that stain weakly and non-uniformly with PH3, and appear be in interphase by DAPI staining. Similar staining patterns have been previously described (Hendzel et al., 1997).
†Excludes 'pre-prophase' cells.
§Standard error between samples.

cells at equivalent stages during later development, it was necessary to use different time points, as *Dm myb* mutants developed more slowly than wild type. Therefore, samples were prepared from wild-type controls at 30 hours APF (roughly equivalent to 42 hours APF in *myb*^{2} mutants; Fig. 2B,E), and from *myb*^{2} and *myb*^{2}/Df(1)*sd*^{72a} at multiple time points, ranging from 40 to 50 hours APF. In addition to proliferating more slowly, mutant *myb* cells continued to divide well beyond 41 hours APF, the time when wild type cells become postmitotic (Madhavan and Madhavan, 1980). Mitotic cells were detected through to at least 50 hours APF in both *myb*^{2} and *myb*^{2}/Df(1)*sd*^{72a} cells (Table 1). In spite of their slower proliferation, at 24 hours APF, the mitotic index of *myb*^{2} histoblasts was similar to that of wild-type cells (Table 1). Surprisingly, the mitotic index of *myb*^{2}/Df(1)*sd*^{72a} cells at 24 hours APF was higher than for *myb*^{2} or controls, and it remained higher throughout the experimental time course. The relatively high mitotic indices in *myb*^{2}/Df(1)*sd*^{72a} cells, which are proliferating so slowly, is indicative of delayed progress through mitosis.

We also analyzed the percentage of cells in S-phase, as judged by 5-bromo-2-deoxyuridine (BrdU) incorporation, and

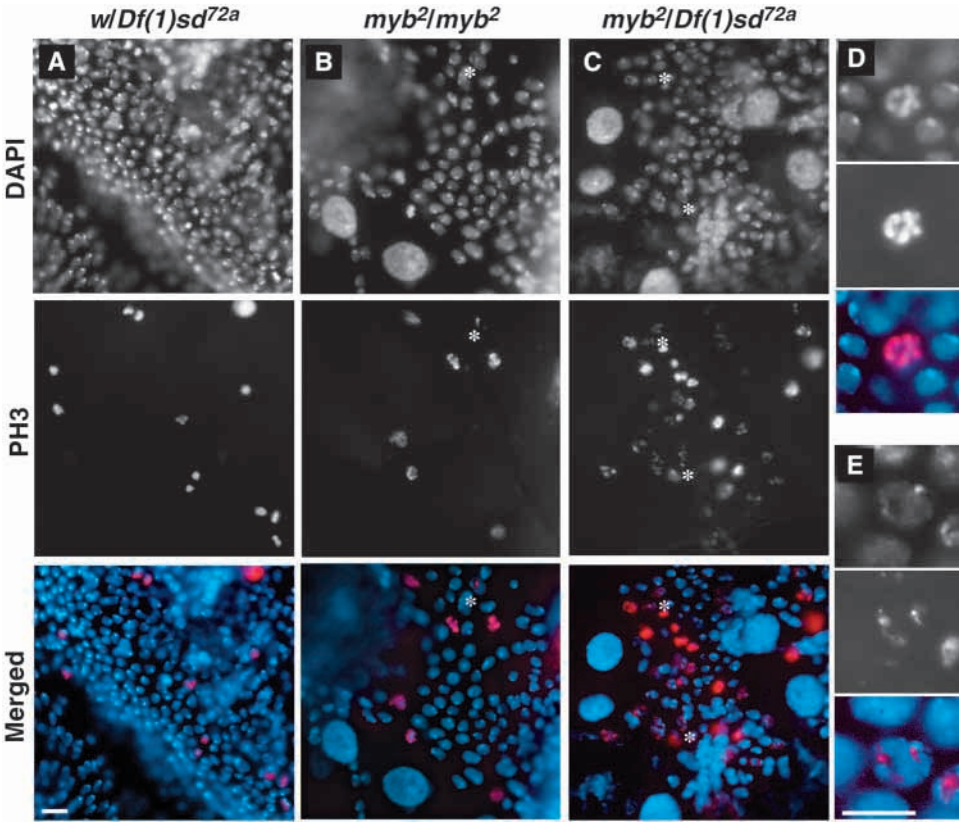

Fig. 3. Chromosome condensation is delayed in abdominal histoblasts that are mutant for *Dm myb*. Abdominal epidermal samples from females were doubly stained with DAPI to visualize nuclei (blue in merged panels) and with the PH3 antibody to identify mitotic cells (red in merged panels, but appearing as magenta because of superimposition on blue). Scale bars: in A, 0.01 mm for A-C; in E, 0.01 mm for D,E. (A,D) *w*/Df(1)*sd*^{72a} controls at 36 hours APF; (B) *myb*^{2} at 36-42 hours APF; (C,E) *myb*^{2}/Df(1)*sd*^{72a} at 42-47 hours APF. Asterisks in (B,C) indicate examples of 'pre-prophase' cells. For comparison, examples of prophase (D) and 'pre-prophase' (E) cells are shown at higher magnification.

Table 2. The percentage of abnormal mitoses in mutant *myb* abdominal histoblasts increased during development

	Metaphase		Anaphase/telophase		All mitotic cells (excluding those in prophase)	
Hours APF	Number of cells examined	% abnormal†	Number of cells examined	% abnormal†	Number of cells examined	% abnormal†
w/Df(1)sd^{72a}						
27-42 hours	487	0%	434	0.2%	921	0.1%
w, myb^2/w, myb^2						
27-32 hours	572	1%	533	3%	1105	2%
36-40 hours	258	2%	139	5%	397	3%
42-45 hours	159	4%	84	10%	243	6%
47-50 hours	25	12%	7	57%	32	22%
w, myb^2/Df(1)sd^{72a}						
27-32 hours	209	0.5%	127	3%	336	2%
36-40 hours	27	2%	73	14%	208	6%
42-45 hours	57	18%	24	33%	81	22%
47-50 hours	37	43%	34	53%	71	48%

†Mitoses were scored as abnormal if they displayed abnormalities in centrosome numbers, mitotic spindles (invariably reflecting aberrant numbers of centrosomes), and/or choursomosomal morphology. (see Fig. 4 and Fig. 7 for examples).

found no significant difference in either the total percentage of cells in S-phase or in the percentage of cells in late S (at which point BrdU labeling is confined to chromocenters) (Lilly and Spradling, 1996) between wild type and mutant cells at 24 hours APF (not shown). As mutant *myb* histoblasts proliferate more slowly than wild type, this finding indicates that S-phase is also lengthened in the mutant cells. The percentage of cells in S-phase decreased in all genotypes at later timepoints, albeit more slowly in mutant cells, a result that is in accordance with their extended proliferation. No conclusions could be drawn about the effects of *myb* mutations on the gap phases as it was not possible in these samples to determine the percentage of cells in G_1 or G_2.

The distribution of cells between the various stages of mitosis was significantly different between *myb* mutants and controls (Table 1). Most notably, there was a higher percentage of mutant cells in the early stages of mitosis, before metaphase, and a corresponding decrease in the percentage of cells in metaphase and anaphase. The number of cells in telophase may be an underestimate as rapid dephosphorylation of histone H3 during telophase makes the PH3 antibody useful for identifying cells in early telophase only (Hendzel et al., 1997; Su et al., 1998). Nevertheless, the percentage of mitotic cells in telophase was lower in *Dm myb* mutant cells (4% of all scored mitoses in either *myb*^{2} or *myb*^{2}/Df(1)*sd*^{72a}) than in wild type (11% of all scored mitoses).

Along with the intense PH3 staining patterns characteristic of prophase, metaphase and anaphase, another pattern was observed in many mutant *myb* cells (Fig. 3). In these cells, the PH3 signal was weaker than is usually observed in wild-type cells, and the chromatin was only partially stained. These nuclei appeared to be in interphase by DAPI staining, but the regions corresponding to the PH3 fluorescent signal also stained more intensely with DAPI, suggesting the onset of chromosome condensation. This PH3 staining pattern has been previously described, and apparently represents a 'pre-prophase' stage that corresponds to the initiation of histone H3 phosphorylation at the G_2/M transition (Hendzel et al., 1997). In wild-type cells, this stage must progress rapidly, as it is rarely observed (1% or less of PH3 staining cells). In mutant cells, however, the frequency of pre-prophase cells increases as pupation proceeds, reaching as high as 30% of all PH3 staining cells in *myb*^{2} and over 40% in *myb*^{2}/Df(1)*sd*^{72a} (Table 1). To determine whether the increase in the pre-prophase staining pattern might be characteristic of cells that continue to divide past the normal cessation of proliferation, we stained abdomens prepared from the *Minute* mutant, *RpS3*^{1} (also known as *M(3)95A*^{1}) (Andersson et al., 1994; Lindsley and Zimm, 1992), with the PH3 antibody. Although mitotic cells were observed through 50 hours APF in this mutant, an increase in pre-prophase cells was not evident (not shown). Therefore, we conclude that the progression of mutant *Dm myb* cells through the early stages of prophase is abnormally slow.

Centrosome abnormalities in *Dm myb* mutant histoblasts

The indications that mutant *Dm myb* abdominal histoblasts progress slowly through mitosis prompted us to examine mitotic cells for cytological defects. Centrosomes were detected using two polyclonal rabbit antibodies raised against

Table 3. Most aberrant mitoses in *Dm myb* mutants contained abnormal numbers of centrosomes

Genotype	% of abnormal mitoses that contained less or more than two centrosomes*	% of cells with three centrosomes†	% of cells with four centrosomes†	Range of centrosome number per cell†	Average number of centrosomes per cell†
w, myb^2/w, myb^2	91%	42%	42%	1-6	3.7
w, myb^2/Df(1)sd^{72a}	71%	38%	36%	1-8	3.8

*The balance of abnormal mitoses contained two centrosomes, but displayed abnormalities in chromosomal morphology.
†Out of the mititic cells with more or less than two chromosomes.

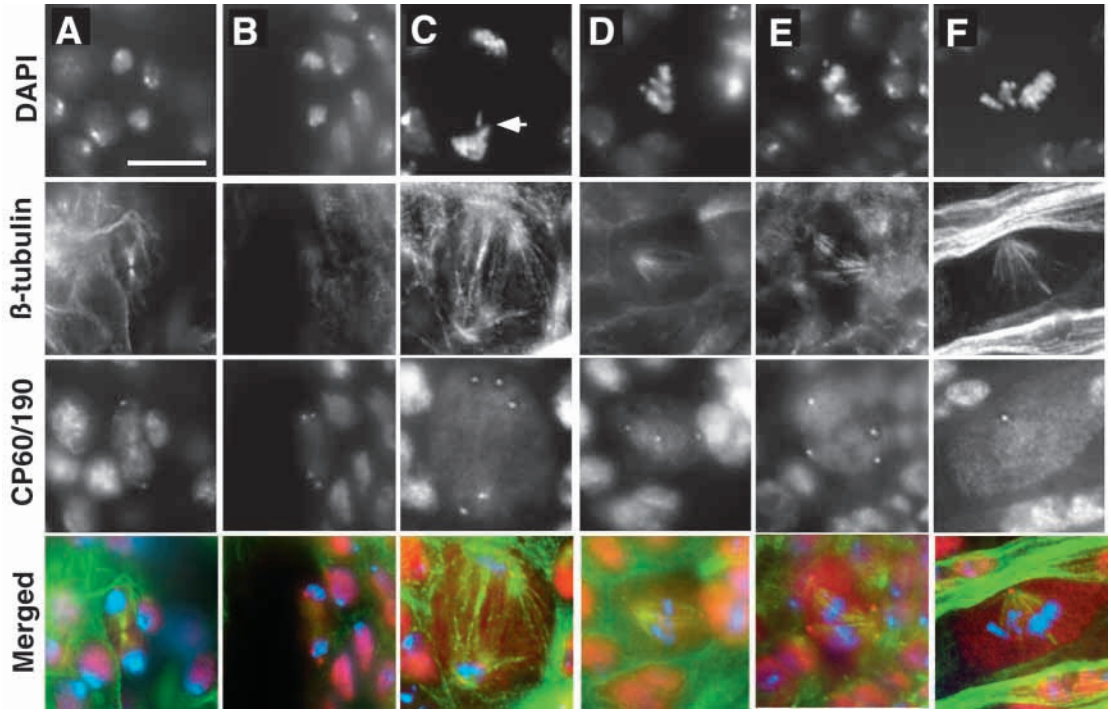

Fig. 4. Most defective mitoses in abdominal histoblasts that are mutant for *Dm myb* display an aberrant number of centrosomes with abnormal spindles and nuclear morphology. Abdominal epidermal samples from females were treated with DAPI to visualize nuclei (blue in merged panels), and immunostained with antibodies against β-tubulin (green in merged panels) and against two centrosomal proteins, CP60 and CP190 (red in merged panels). Interphase nuclei appear magenta in merges due to combined signal from DAPI and the nuclear CP60/190 proteins. Scale bar in A: 0.01mm. One centrosome was visible at each pole in control cells during anaphase (A) *w*/Df(1)*sd*^{72a}, 40 hours APF; whereas two centrosomes were frequently seen at each pole in *Dm myb* mutant homozygotes (B) *myb*^{2}, 44 hours APF. (C-F) Additional representatives of mutant cells with abnormal numbers of centrosomes. (C) *myb*^{2}/Df(1)*sd*^{72a}, 48 hours APF, five centrosomes; relatively normal anaphase with evidence of straggling DNA (arrow). (D) *myb*^{2}/Df(1)*sd*^{72a}, 48 hours APF, three centrosomes; disrupted organization of spindles and chromosomes during metaphase. (E) *myb*^{1}/Df(1)*sd*^{72a}, 67 hours APF at 18°C, four centrosomes; two metaphase plates. (F) *myb*^{2}, 42 hours APF, one centrosome organizing a monopolar spindle.

previously described centrosomal proteins, CP60 and CP190, both of which localize to the centrosome during mitosis and are otherwise nuclear (Kellogg and Alberts, 1992; Kellogg et al., 1995; Whitfield et al., 1988). Antibodies raised against two other centrosomal proteins, γ-tubulin and centrosomin (Heuer et al., 1995), produced similar results. A monoclonal rat antibody raised against β-tubulin was used to visualize the microtubule spindle.

Although histoblast proliferation was slower in *Dm myb* mutants throughout pupal development, mitotic defects were not detected in early divisions (up to 24 hours APF), but became increasingly commonplace later (Table 2). No defects were observed in greater than 99% of wild-type mitoses, whereas abnormalities occurred in as many as 22% of *myb*^{2} and 48% of *myb*^{2}/Df(1)*sd*^{72a} mitotic histoblasts. One defect, in which two centrosomes were present at, or near each pole during anaphase/telophase (Fig. 4B), occurred more frequently in *myb*^{2} (and *myb*^{1}) abdominal histoblasts than in *myb*^{2}/Df(1)*sd*^{72a}, indicating it might be the mildest. Mitotic spindles with two centrosomes at each pole were seen much less frequently in metaphase and early anaphase cells. Therefore, we suspect that this defect reflects precocious separation of the centriole pairs associated with each centrosome. Disengagement of mother and daughter centrioles has been reported to occur during late anaphase/early telophase in *Drosophila* embryos (Gonzalez et al., 1998; Vidwans et al., 1999), but no signs of separation were detected in wild-type histoblasts (Fig. 4A).

The majority of mitotic abnormalities were associated with aberrant numbers of centrosomes, ranging from one to eight, with the most common numbers being three or four (Table 3; Fig. 4). Most, if not all of the supernumerary centrosomes nucleated mitotic spindles. When the additional centrosomes were located at, or near each pole, a bipolar spindle was still

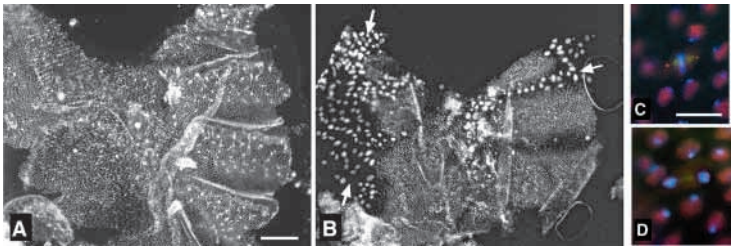

Fig. 5. Ectopic expression of RBF delayed proliferation of abdominal histoblasts, but did not result in abnormal numbers of centrosomes during mitosis. White prepupae from either UAS-RBF alone as a control (A) or hsp70-GAL4/UAS-RBF (B-D) were picked and subjected to a 40 minute heat shock at 37°C. Heat shock treatment was repeated every 12 hours until pupae were dissected at 40-43 hours APF. Samples were treated with DAPI to visualize nuclei (A,B, and blue in merged panels), and immunostained with antibodies against β-tubulin (green in merged panels) and two centrosomal proteins, CP60 and CP190 (red in merged panels). Low magnification views show normal development of the heat shocked UAS-RBF control (A) and the developmental delay caused by ectopic expression of RBF (B). Arrows indicate areas where larval polyploid cells have not been replaced by histoblasts. Representative metaphase (C) and anaphase (D) nuclei from the delayed mitoses have appropriate numbers of centrosomes. Scale bar: in A, 0.1 mm for A,B; in C, 0.01 mm for C,D

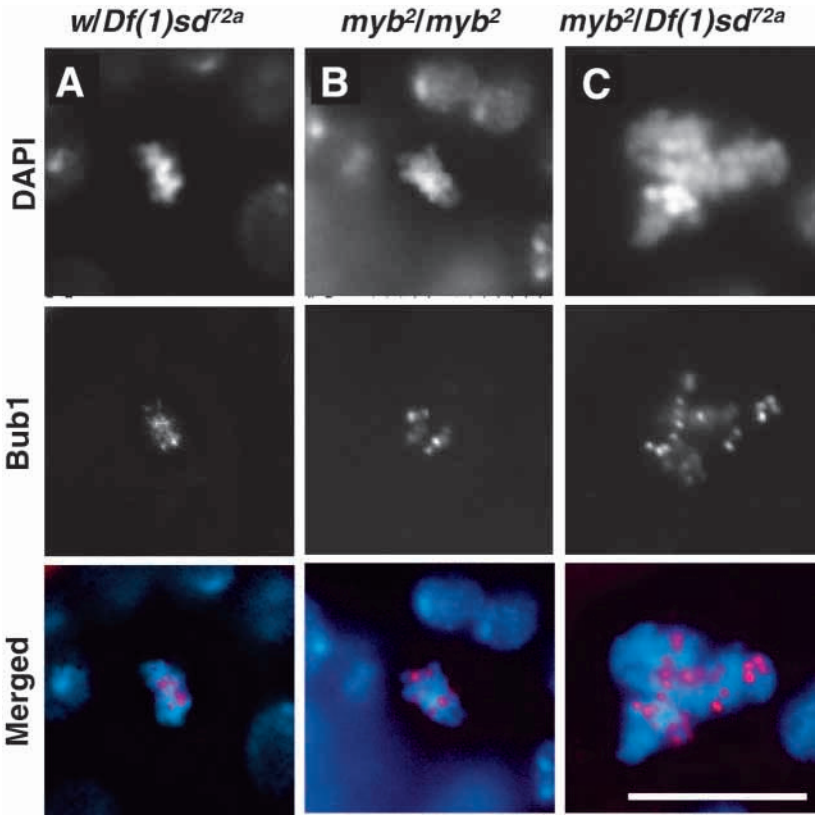

Fig. 6. Chromosomal dynamics are disturbed during mitosis in mutant *Dm myb* abdominal histoblasts. Abdominal epidermal samples from females were doubly stained with DAPI to visualize nuclei (blue in merged panels) and with antibodies against the kinetochore associated protein, Bub1 (red in merged panels). (A-C) Mutations in *Dm myb* disturbed kinetochore arrangement during metaphase. (A) *w*/Df(1)*sd*^{72a} control, 24 hours APF. (B) *myb*^{2}, 42 hours APF. (C) The presence of more than 16 Bub1 signals in this *myb*^{2}/Df(1)*sd*^{72a} cell (42 hours APF) is indicative of polyploidy and demonstrates that such cells continue to progress into mitosis. Scale bar: 0.01 mm.

formed allowing for chromosome separation (Fig. 4C). More commonly, extra centrosomes formed multipolar spindles, pulling chromosomes in multiple directions (Fig. 4D,E). When a large number of centrosomes were distributed throughout the cell, a proper spindle apparatus was not formed (not shown). Cells with single centrosomes organizing monopolar spindles were occasionally seen (Fig. 4F). Chromosomal abnormalities were common in mitotic cells with aberrant centrosome numbers (Fig. 4), but were also observed in mitotic cells containing two centrosomes (Table 3).

Two approaches were taken to determine whether mitotic defects are characteristic of cells that continue to divide past the normal cessation of proliferation. First, samples were prepared from two *Minute* mutants, *RpS3*^{1} and *M(3)65F*^{1} (Andersson et al., 1994; Lindsley and Zimm, 1992), at 42 and 50 hours APF. Out of 61 mitotic cells examined, no abnormalities were found. However, *Minute* mutants may not provide an ideal control as these mutations lead to a generalized slowing of proliferation throughout development owing to decreased protein synthesis. Therefore, we used the GAL4/UAS binary system to induce ectopic expression of the *Drososphila* retinoblastoma-family protein (RBF), a negative regulator of cell cycle progression (Du and Dyson, 1999). We chose to use the hsp70-GAL4 driver to induce ectopic expression during pupal development. Although heat shock treatment will induce UAS-RBF expression in all cells, it should have a particularly strong effect on abdominal histoblasts during early pupation at a time when these cells divide rapidly (as opposed to imaginal disc cells which have completed most of their divisions before this stage). Ectopic expression of RBF significantly delayed abdominal development (Fig. 5A,B). For control abdomens (UAS-RBF alone), only five mitoses were detected in eight abdominal preparations (dorsal surface only; no mitoses were observed in ventral surface, but muscles make the analysis difficult at this stage). By contrast, 122 mitoses were found and examined in the dorsal surface of only three abdominal preparations from the experimental samples (43 more mitoses detected on the ventral surface). No abnormalities in centrosome number or spindle morphology were detected in these dividing cells (Fig. 5C,D). We conclude that delaying the cell cycle via RBF expression does not lead to centrosomal/spindle defects, demonstrating that the defects observed in the *myb* mutants are not merely a secondary event of delayed cell cycle progression.

Metaphase cells with lagging chromosomes were observed much more often in *Dm myb* mutants than in wild-type controls (see Fig. 4D). When we used an antibody against the mitotic checkpoint control protein Bub1, which localizes most strongly to the kinetochore of mitotic chromosomes that have not yet reached metaphase plate (Basu et al., 1999), we found that kinetochores were less uniformly arranged in mutant than wild-type cells, even when all chromosomes appeared to be lined up at the metaphase plate (Fig. 6A,B). In some mutant cells, we observed more than the 16 kinetochores that should be present in a mitotic *Drosophila* cell, indicating that these cells were polyploid and/or aneuploid, and that they were continuing to progress through the cell cycle (Fig. 6C). Another chromosomal defect was the presence of more than one metaphase plate in a single cell (Fig. 4E). During anaphase, straggling strands of DNA were frequently observed (Fig. 4C). However, there was no significant Bub1 staining in anaphase cells, regardless of DNA morphology (not shown), indicating that APC pathways were not grossly disturbed in *Dm myb* mutants.

Centrosome amplification causes unequal chromosome segregation, resulting in aneuploidy and polyploidy

How are the abnormal mitoses with extra centrosomes forming multipolar spindles in *myb* mutants resolved? Do they apoptose, become trapped in metaphase indefinitely, complete division and form multiple daughter cells with unbalanced chromosome segregation or return to an interphase state? A definitive answer is difficult as mitoses in abdominal histoblasts cannot be readily monitored in vivo. However, the first two possibilities appear to be rare, because neither elevated

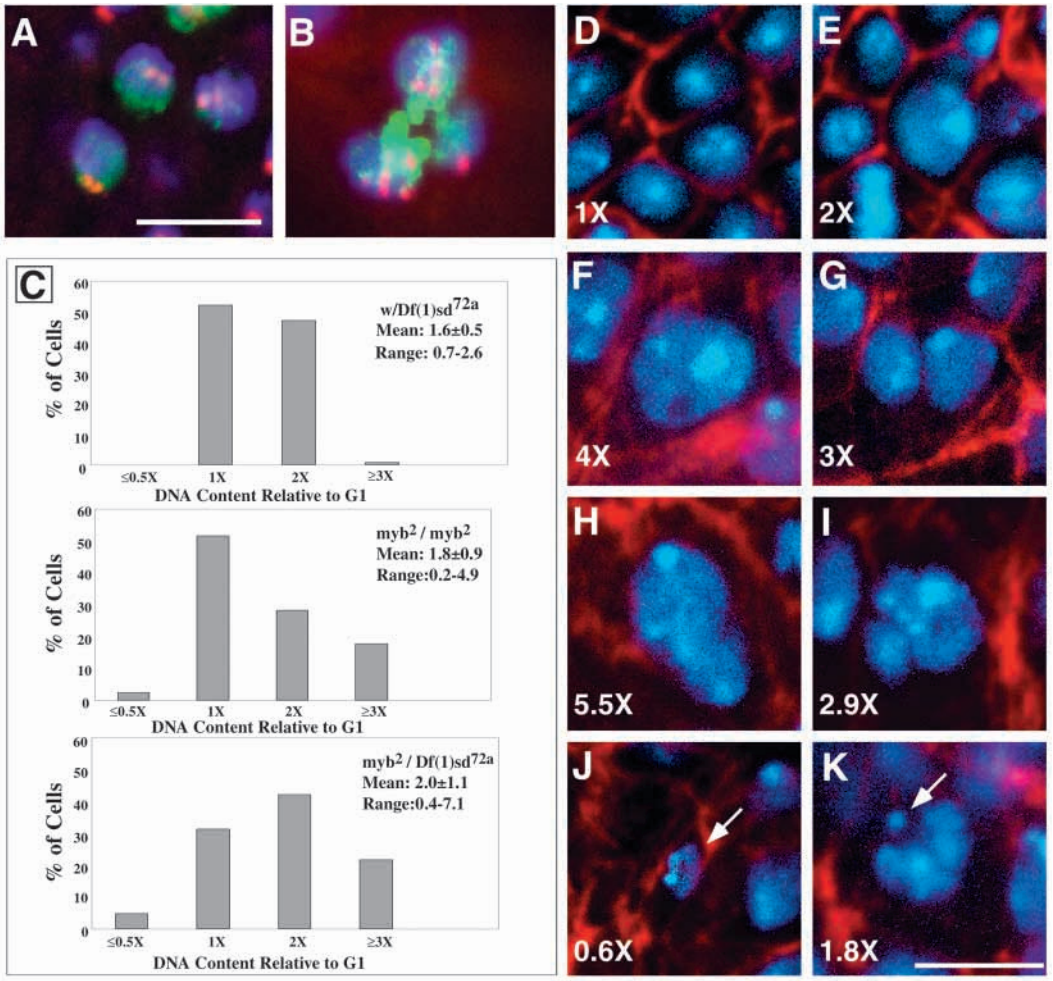

Fig. 7. Aneuploidy, polyploidy and variable nuclear morphology in mutant *Dm myb* abdominal epidermal cells. (A,B) Abdominal epidermal samples from female pupae hybridized with an X-chromosome probe (red), and stained with DAPI (blue) and PH3 antibodies (green). (A) Two signals were seen in each of two separating nuclei in *w*/Df(1)*sd*^{72a} controls during anaphase. (B) By contrast, a different number of signals (1, 4 and 6) were evident in each of three separating nuclei in a mutant *myb*^{2} cell. (C-K) Abdominal epidermal samples from females at 30 hours APF for controls and at 44-46 hours APF for *Dm myb* mutants were stained with DAPI for DNA quantitation (blue in D-K) and rhodamine-labeled phalloidin (red in D-K), and optically sectioned by confocal microscopy under identical conditions. For each of three experiments, nuclear fluorescent intensities were measured. The average value of the G_1 control nuclei was determined and used as the base value of 1×. Values of other nuclei were adjusted accordingly to calculate relative fluorescent intensities. (C) Results of analyzing 121 control (*w*/Df(1)*sd*^{72a}); 124 *myb*^{2}, and 83 *myb*^{2}/Df(1)*sd*^{72a} nuclei are graphically represented. The range of values included in each category are indicated in parentheses as follows: ≤ 0.5× (≤ 0.6); 1× (0.7-1.5×); 2× (1.6-2.5×) and ≥ 3× (≥ 2.6). (D-K) Examples of control and mutant cells with relative DNA quantitation values as indicated. (D) Three control *w*/Df(1)*sd*^{72a} G_1 nuclei; (E) a control G_2 nucleus is centered; (F) enlarged *myb*^{2} nucleus; (G) binucleate *myb*^{2} cell; (H) mis-shapen and enlarged *myb*^{2}/Df(1)*sd*^{72a} nucleus; (I) multilobed *myb*^{2}/Df(1)*sd*^{72a} nucleus; (J) a *myb*^{2}/Df(1)*sd*^{72a} nucleus with subdiploid DNA content (arrow); (K) a *myb*^{2}/Df(1)*sd*^{72a} cell containing a large nucleus and a micronucleus indicated by arrow. Scale bars: in A, 0.01 mm in A,B; in K, 0.01 mm in D-K.

levels of apoptosis nor ever increasing levels of metaphase chromosomes were observed. The lack of increased apoptosis was surprising given the severity of mitotic defects and evidence that vertebrate Myb genes can suppress apoptosis (Frampton et al., 1996; Taylor et al., 1996), thereby raising the possibility that apoptosis may be suppressed in abdominal epidermal cells.

When a probe representing a 359 bp repeat present in X-chromosome heterochromatin (Dernburg, 2000), was used for FISH on samples prepared from females, two signals were detected in each daughter nucleus during mitosis (Fig. 7A). In *myb* mutants, cells with tripolar spindles that progressed to anaphase were occasionally observed. Fig. 6B shows an example in which each of the three daughter nuclei displayed a different number of signals, ranging from one to six, demonstrating unequal chromosome segregation, and confirming that some mutant polyploid cells continued to divide with dire consequences for genomic integrity. No example of mitoses forming more than three daughter cells was observed, suggesting that cells with four or more poles never complete mitosis. Instead, we suspect the chromosomes decondense and eventually take on the appearance of interphase nuclei, albeit with abnormal morphology (see below).

To compare cell size, nuclear morphology and DNA content between wild-type and mutant *myb* abdominal epidermal cells, samples were stained with DAPI and rhodamine-labeled phalloidin. We were unable to examine postmitotic cells because the mutant epidermal cells were still proliferating at the latest time point for which we could prepare samples (50 hours APF). Therefore, the analysis was performed on mutant samples prepared at 44-46 hours APF and on control samples at 30 hours APF, a time point when wild-type cells are also still proliferating (see Table 1). Mutant *myb*^{2} cells and nuclei were often larger than wild type, and cells with either two fused or separated nuclei were occasionally observed (Fig. 7F,G). Both features were more pronounced in *myb*^{2}/Df(1)*sd*^{72a} cells, but these cells also exhibited more variability in size, with nuclei that were often abnormally shaped and/or multilobed (Fig. 7H,I). The mitotic defects, however, did not necessarily

result in polyploidy. Mutant cells with subdiploid nuclei or that contained a micronucleus in addition to a larger nucleus were also detected (Fig. 7J,K).

To assess relative DNA contents (Fig. 7C), we measured the relative fluorescent intensities of DAPI-stained nuclei from a series of confocal images (see Materials and Methods). DNA content was calculated on a per cell basis, regardless of nuclear morphology or the presence of more than one nucleus. As expected for proliferating cells, the DNA content of control cells varied over a twofold range, with only 1 of 121 nuclei falling slightly outside the one- to twofold range. By contrast, both the average and range of DNA contents were larger for mutant *Dm myb* cells than for wild type, with more than 20% of myb^2 and 25% of myb^2/Df(1)sd^{72a} nuclei falling outside the one- to twofold range. These figures are likely to be an underestimate, as several of the larger mutant nuclei could not be measured because they were not entirely contained within the *z*-stack of optical sections. The mitotic defects observed in the mutant cells (see Fig. 4, Fig. 5, Fig. 7) indicate that some of the cells within the one- to twofold range were likely to be aneuploid. Variability was especially pronounced in myb^2/Df(1)sd^{72a} cells, where small nuclei were occasionally seen that contained less than diploid levels of DNA (approximately half, Fig. 7J), while other nuclei had DNA contents that ranged as high as sevenfold more than the normal diploid levels in wild-type cells. Our results confirm that the abnormal mitoses occurring in *Dm myb* mutant histoblast cells give rise to unequal chromosome segregation and produce aneuploid and polyploid nuclei.

To investigate whether nuclear morphology abnormalities and polyploidy were already apparent by the time the first centrosomal defects were observed, control and mutant samples at 28-30 hours after puparium formation were prepared as described above. Greater than 100 control and 175 mutant cells (myb^2 and myb^2/Df(1)sd^{72a} combined) were examined. No examples of cells with either two nuclei or a multilobed nucleus were observed at this stage of development. The DNA content of more than 98% of control and mutant cells varied over the same twofold range as was previously observed for control cells at 30 hours APF. These data indicate that the observed centrosome abnormalities are unlikely to arise from failure to complete mitosis or cytokinesis as these defects do not precede the centrosome defects.

DISCUSSION

Distinctions between wing and abdominal phenotypes in *Dm myb* mutants

In previous analysis of the mutant *Dm myb* wing phenotype, we found that wing cells were arrested in G_2 of their final cell cycle during pupal development, and that some of the arrested cells had entered into endoreduplication, indicating that *Dm myb* is required for both promotion of the G_2/M transition and suppression of endoreduplication (Katzen et al., 1998). While current studies of the abdominal phenotype also display defects in cellular proliferation, there are several distinctions in the specific defects observed, revealing that *Dm myb* function is required not only to enter mitosis, but to proceed through mitosis. Discrepancies cannot be rationalized by differences in mutations, as the same alleles were used for both studies. Instead, new aspects of *Dm myb* function may be revealed in abdominal histoblasts because of the demands of their developmental program. Histoblasts proliferate more rapidly than wing cells (doubling times of less than 3 hours versus 10-12 hours for wing cells) (Madhavan and Madhavan, 1980), and the levels of *Dm myb* mRNA are lower in histoblasts than in wing discs (Katzen and Bishop, 1996). Comparison of developmental delays indicates that abdominal histoblasts are indeed more sensitive to reductions in *Dm myb* function. In *Dm myb* mutants, wing development only lagged behind wild type by about 1.5 hours (Katzen et al., 1998), whereas abdominal development lagged by 10 to 12 hours. It is also possible that additional mitotic functions for *Dm myb* are revealed in abdominal cells because regulation of the G_2/M transition is not as restrictive as it is in wing cells.

Defects in *esg* and *cdc2* mutants have been attributed to a failure to suppress endoreduplication in abdominal histoblasts during larval development when they are normally arrested in G_2 (Hayashi, 1996; Hayashi et al., 1993). Although the abdominal phenotype in *Dm myb* mutants resembles those of *esg* and *cdc2* (Hayashi et al., 1993; Stern et al., 1993), mutant *Dm myb* histoblast nests contain appropriate numbers of cells with no apparent abnormalities. This indicates that although *Dm myb* function appears to be required to suppress endoreduplication during an aberrant G_2 arrest, it is not essential for keeping abdominal histoblasts in the normal extended G_2 phase that persists throughout larval development.

In previous analyses of the mutant *myb* phenotype, the myb^1 allele inevitably produced a stronger phenotype than myb^2 at equivalent temperatures (Katzen and Bishop, 1996; Katzen et al., 1998). By contrast, the abdominal phenotype is as strong or stronger in myb^2 than in myb^1 at the same temperatures (see Fig. 1, Fig. 2), indicating that the relationship between the two temperature-sensitive alleles is more complex than previously thought. Although each mutation results in the change of an amino acid perfectly conserved between Myb and its vertebrate counterparts, different regions of the protein are affected: for myb^2, the DNA-binding domain; and for myb^1, a conserved domain (region IV) near the C terminus for which no specific biochemical activity has yet been ascribed (Katzen et al., 1998). The finding that the myb^1 phenotype is stronger than myb^2 in wing cells, but weaker in abdominal cells indicates that Myb activity is differentially regulated in these two tissues.

Analysis of the abdominal phenotype in myb mutants expands our understanding of Dm myb function in mitosis

Although several abnormalities are observed in *Dm myb* mutant abdominal histoblasts, the earliest developmental defects are likely to represent the primary cellular defect. Abdominal histoblast cells in *Dm myb* mutants appeared normal during larval development, a period during which they are arrested in G_2, but their rate of proliferation after puparium formation was considerably slower than for wild-type cells. The sluggish proliferation did not correlate with a commensurate decrease in mitosis. For example, although histoblasts in myb^2/Df(1)sd^{72a} animals lagged behind wild-type cells by two to three cell division cycles, the mitotic index in the mutants was considerably higher (5.7% versus 2.7% at 24 hours APF), indicating that at least part of the reduced rate

of proliferation in mutants can be attributed to abnormally slow progression through mitosis.

Examination of the mitotic cells revealed an enrichment of cells in the early stages of mitosis (pre-metaphase; see Table 1). Even at 24 hours APF, there is an increased ratio of prophase to metaphase cells, and as development proceeds, an increasing number of cells stall in pre-prophase. Whether the majority of pre-prophase cells ever proceed further into mitosis is unclear. It is also possible that some of the weakly staining PH3 cells were not in pre-prophase, but were instead undergoing chromosome decondensation after having failed to complete mitosis or cytokinesis. We believe these are likely to be in the minority for several reasons: an increased percentage of pre-prophase cells can be seen as early as 24 hours APF, before other mitotic or ploidy abnormalities are evident. Up until 30 hours APF, double staining with rhodamine-labeled phalloidin and DAPI revealed an absolute correspondence of one nucleus per cell. In addition, weakly staining PH3 cells did not have abnormally shaped nuclei, even at later developmental timepoints, as did most cells that failed to complete mitosis; instead, the morphology and PH3 staining of the pre-prophase nuclei closely resembled those shown by Hendzel et al. (Hendzel et al., 1997) and the occasional pre-prophase nuclei that we observed in wild-type cells. One further possibility, which cannot be ruled out at present, is that the regulation of histone H3 phosphorylation is somewhat abnormal in these cells, and therefore, the weak staining may not always reflect pre-prophase. Our scoring of mitotic cells did not distinguish between prometaphase and metaphase, but the Bub1 staining patterns suggest that in the mutants, the 'metaphase' population is likely to be enriched for prometaphase cells. Therefore, we conclude that *Dm myb* mutant histoblasts appear to suffer delays or partial blocks in chromatin condensation, in the process of kinetochore attachment to the mitotic spindle and in chromosome alignment on the metaphase plate.

The percentage of *Dm myb* mutant histoblasts with visible mitotic abnormalities increases dramatically as pupal development proceeds, implying that initial defects are compounded in subsequent divisions. These mitotic defects, which include aberrant numbers of centrosomes, grossly abnormal DNA morphology, aneuploidy and polyploidy, are characteristic of situations in which the coordination of centrosome and nuclear cycles has been disturbed. Failure to precisely coordinate centrosome doubling with the nuclear cell cycle produces mitotic cells with less than or greater than two centrosomes, a situation that generally results in the formation of abnormal spindles (Sluder and Hinchcliffe, 1999). Examples of such abnormalities, which inevitably lead to genomic instability, are represented among *Dm myb* mutant abdominal cells. Mitotic cells with only one centrosome forming a monopolar spindle are occasionally seen. These cells cannot divide and will inevitably produce polyploid cells. More commonly observed are mitotic cells with more than two centrosomes forming multipolar spindles. In such a situation, chromosomes will be randomly distributed into multiple daughter cells which will be aneuploid if cell division is successfully completed. Alternatively, if the mitotic cell fails to complete division and returns to an interphase state, the resulting cell would either be multinucleate or contain a single polyploid nucleus. Our results indicate that all of these possible outcomes occur in mutant *Dm myb* cells. Therefore, we believe that defects observed during later stages of abdominal epidermal development are the consequence of disturbing the coordination between centrosome reproduction and the nuclear cell cycle.

In a recent study that compared gene expression in actively proliferating fibroblasts isolated from people of different ages or from individuals with the premature aging disease progeria, *Mybl2* expression was significantly downregulated in both progeria fibroblasts and in 'normal' fibroblasts isolated from old-aged (~90 years) people (Ly et al., 2000). A significant proportion of these 'aged' fibroblasts exhibited abnormalities, including multilobed nuclei and multiple nuclei within a cell. These nuclear defects are reminiscent of those observed in the abdominal epidermal cells of *Dm myb* mutants, suggesting the possibility that reduced levels of *Mybl2* might lead to centrosomal abnormalities, which in turn cause aneuploidy and polyploidy.

Is the disturbance in centrosome regulation a primary defect of the mutation in *Dm myb* or a secondary consequence of the slow rate of proliferation and/or delays in early mitotic stages, which occur earlier in development? Our analysis indicates that the centrosome defect may be primary, as the first abnormalities in centrosome numbers precede the appearance of multilobed and binucleated cells, allowing us to exclude the possibility that a failure in mitosis or cytokinesis represents the primary defect. Once present, however, the extra centrosomes do lead to defective mitoses and failed cell divisions.

Many links have been established between the regulation of the cell division cycle and centrosome duplication. Artificial prolongation of mitosis leads to premature splitting and separation of centrosomes, while prolongation of S-phase allows multiple rounds of centrosome duplication to occur (Sluder and Hinchcliffe, 1999). The mildest centrosome defect in *Dm myb* mutants appears to be a premature separation of centriole pairs during late anaphase/early telophase, which could be the result of delayed progression through mitosis. Premature separation might explain why the percentage of centrosome abnormalities is always higher in anaphase/telophase cells than in metaphase cells (see Table 2). This early separation may therefore represent the first step in a breakdown of the coordination between nuclear and centrosome cell cycles.

Another indication that splitting and/or duplication of centrosomes is not occurring in a coordinated fashion is the frequent occurrence of odd numbers of centrosomes within the mutant cells. Four centrosomes in mutant cells could result from failure to complete the previous cell division, followed by re-entry into the cell cycle. A subsequent mitosis could then easily lead to an assortment of an odd number of centrosomes in each daughter cell (e.g. three in one and one in the other), but they should be duplicated during the subsequent cycle, thereby generating an even number by the following mitosis (six and two, respectively). Intriguingly, odd numbers of centrosomes are also a common feature in vertebrate cells that have suffered a mutation in a tumor suppressor gene such as *p53*, *Brca1* or *Brca2* (Fukasawa et al., 1996; Tutt et al., 1999; Xu et al., 1999).

Can Myb genes function as both oncogenes and tumor suppressor genes?

The normal function of many proto-oncogenes is to participate in signal transduction pathways that regulate cellular

proliferation. When proto-oncogenes suffer mutations that convert them to activated oncogenes, they promote uncontrolled cell growth. Specific aspects of the phenotypic defects observed in the *Dm myb* mutants, such as sluggish proliferation and stalling or arresting at the G_2/M transition, match expectations for loss-of-function mutations in a proto-oncogene. Centrosome amplification and genomic instability, however, are frequently associated with loss-of-function mutations in tumor suppressor genes, not proto-oncogenes (Fukasawa et al., 1996; Tutt et al., 1999; Xu et al., 1999). As genomic instability is associated with oncogenic progression and aggressive tumors, the disturbance in the regulation of centrosome reproduction may be the primary mechanism by which tumorigenesis is promoted when some tumor suppressor genes are mutated (Sluder and Hinchcliffe, 1999; Tutt et al., 1999; Xu et al., 1999). Therefore, the *Dm myb* gene shares some properties with proto-oncogenes and others with tumor suppressor genes, raising the possibility that mutations which decrease the activity of one of the vertebrate Myb genes could contribute to genomic instability and subsequent oncogenesis or aging.

We thank Michelle Moritz and Jordan Raff for supplying CP60 and CP190 antibodies; Meg Bentley and Michael Goldberg for Bub1 antibodies; Tom Kaufmann for centrosomin antibodies; Shigeo Hayashi and Bruce Edgar for fly stocks; Randal Cox for troubleshooting assistance when image processing or computer difficulties arose; Rob Costa for use of his dissecting microscope and imaging system for adult abdomens; and J. Michael Bishop and Pat O'Farrell for useful suggestions. We are grateful to Tin-Tin Su for many insightful suggestions, for supplying the probe and protocol for FISH experiments, and for critical reading of the manuscript. Work reported here was supported by a National Institutes of Health grant to A. L. K. (CA74221).

REFERENCES

Andersson, S., Saeboe-Larssen, S., Lambertsson, A., Merriam, J. and Jacobs-Lorena, M. (1994). A Drosophila third chromosome Minute locus encodes a ribosomal protein. *Genetics* **137**, 513.

Audibert, A., Debec, A. and Simonelig, M. (1996). Detection of mitotic spindles in third-instar imaginal discs of Drosophila melanogaster. *Trends Genet.* **12**, 452.

Basu, J., Bousbaa, H., Logarinho, E., Li, Z., Williams, B. C., Lopes, C., Sunkel, C. E. and Goldberg, M. L. (1999). Mutations in the essential spindle checkpoint gene bub1 cause chromosome missegregation and fail to block apoptosis in Drosophila. *J. Cell Biol.* **146**, 13.

Bishop, J. M., Eilers, M., Katzen, A. L., Kornberg, T., Ramsay, G. and Schirm, S. (1991). MYB and MYC in the cell cycle. *Cold Spring Harb. Symp. Quant. Biol.* **56**, 99.

Chester, N., Kuo, F., Kozak, C., O'Hara, C. D. and Leder, P. (1998). Stage-specific apoptosis, developmental delay, and embryonic lethality in mice homozygous for a targeted disruption in the murine Bloom's syndrome gene. *Genes Dev.* **12**, 3382.

Cohen, S. M. (1993). Imaginal disc development. In *The Development of* Drosophila melanogaster. Vol. II (ed. M. Bate and A. Martinez-Arias), pp. 747. Cold Spring Harbor: Cold Spring Harbor Laboratory Press.

Craymer, L. and Roy, E. (1980). New mutants. *Drosophila Information Service* **55**, 200.

Dernburg, A. F. (2000). In situ hybridization to somatic chromosomes. In Drosophila *Protocols* (ed. W. Sullivan, M. Ashburner and R. S. Hawley), pp. 25. New York: Cold Spring Harbor Laboratory Press.

Du, W. and Dyson, N. (1999). The role of RBF in the introduction of G1 regulation during Drosophila embryogenesis. *EMBO J* **18**, 916.

Euling, S. and Ambros, V. (1996). Heterochronic genes control cell cycle progress and developmental competence of C. elegans vulva precursor cells. *Cell* **84**, 667.

Frampton, J., Ramqvist, T. and Graf, T. (1996). v-Myb of E26 leukemia virus up-regulates bcl-2 and suppresses apoptosis in myeloid cells. *Genes Dev.* **10**, 2720.

Fristrom, D. and Fristrom, J. W. (1993). The metamorphic development of the adult epidermis. In *The Development of* Drosophila melanogaster. Vol. II (ed. M. Bate and A. Martinez-Arias), pp. 843. Cold Spring Harbor: Cold Spring Harbor Laboratory Press.

Fukasawa, K., Choi, T., Kuriyama, R., Rulong, S. and Vande Woude, G. F. (1996). Abnormal centrosome amplification in the absence of p53. *Science* **271**, 1744.

Gao, Y., Ferguson, D. O., Xie, W., Manis, J. P., Sekiguchi, J., Frank, K. M., Chaudhuri, J., Horner, J., DePinho, R. A. and Alt, F. W. (2000). Interplay of p53 and DNA-repair protein XRCC4 in tumorigenesis, genomic stability and development. *Nature* **404**, 897.

Gonzalez, C., Tavosanis, G. and Mollinari, C. (1998). Centrosomes and microtubule organisation during Drosophila development. *J. Cell Sci.* **111**, 2697.

Hartwell, L., Weinert, T., Kadyk, L. and Garvik, B. (1994). Cell cycle checkpoints, genomic integrity, and cancer. *Cold Spring Harb. Symp. Quant. Biol.* **59**, 259.

Hayashi, S. (1996). A Cdc2 dependent checkpoint maintains diploidy in Drosophila. *Development* **122**, 1051.

Hayashi, S., Hirose, S., Metcalfe, T. and Shirras, A. D. (1993). Control of imaginal cell development by the escargot gene of Drosophila. *Development* **118**, 105.

Hayashi, S. and Yamaguchi, M. (1999). Kinase-independent activity of Cdc2/cyclin A prevents the S phase in the Drosophila cell cycle. *Genes Cells* **4**, 111.

Hendzel, M. J., Wei, Y., Mancini, M. A., Van Hooser, A., Ranalli, T., Brinkley, B. R., Bazett-Jones, D. P. and Allis, C. D. (1997). Mitosis-specific phosphorylation of histone H3 initiates primarily within pericentromeric heterochromatin during G2 and spreads in an ordered fashion coincident with mitotic chromosome condensation. *Chromosoma* **106**, 348.

Heuer, J. G., Li, K. and Kaufman, T. C. (1995). The Drosophila homeotic target gene centrosomin (cnn) encodes a novel centrosomal protein with leucine zippers and maps to a genomic region required for midgut morphogenesis. *Development* **121**, 3861.

Jackson, J., Ramsay, G., Sharkov, N. V., Lium, E. and Katzen, A. L. (2001). The role of transcriptional activation in the function of the *Drosophila myb* gene. *Blood Cells Mol. Dis.* **27**, 446.

Karow, J. K., Wu, L. and Hickson, I. D. (2000). RecQ family helicases: roles in cancer and aging. *Curr. Opin. Genet. Dev.* **10**, 32.

Katzen, A. L. and Bishop, J. M. (1996). myb provides an essential function during Drosophila development. *Proc. Natl. Acad. Sci. USA* **93**, 13955.

Katzen, A. L., Jackson, J., Harmon, B. P., Fung, S.-M., Ramsay, G. and Bishop, J. M. (1998). Drosophila myb is required for the G2/M transition and maintenance of diploidy. *Genes Dev.* **12**, 831.

Katzen, A. L., Kornberg, T. B. and Bishop, J. M. (1985). Isolation of the proto-oncogene c-myb from D. melanogaster. *Cell* **41**, 449.

Kellogg, D. R. and Alberts, B. M. (1992). Purification of a multiprotein complex containing centrosomal proteins from the Drosophila embryo by chromatography with low-affinity polyclonal antibodies. *Mol. Biol. Cell* **3**, 1.

Kellogg, D. R., Oegema, K., Raff, J., Schneider, K. and Alberts, B. M. (1995). CP60: a microtubule-associated protein that is localized to the centrosome in a cell cycle-specific manner. *Mol. Biol. Cell* **6**, 1673.

Kopp, A., Muskavitch, M. A. and Duncan, I. (1997). The roles of hedgehog and engrailed in patterning adult abdominal segments of Drosophila. *Development* **124**, 3703.

Lilly, M. A. and Spradling, A. C. (1996). The Drosophila endocycle is controlled by Cyclin E and lacks a checkpoint ensuring S-phase completion. *Genes Dev.* **10**, 2514.

Lindsley, D. L. and Zimm, G. G. (1992). *The genome of* Drosophila melanogaster. San Diego, CA: Academic Press.

Ly, D. H., Lockhart, D. J., Lerner, R. A. and Schultz, P. G. (2000). Mitotic misregulation and human aging. *Science* **287**, 2486.

Madhavan, M. M. and Madhavan, K. (1980). Morphogenesis of the epidermis of adult abdomen of Drosophila. *J. Embryol. Exp. Morphol.* **60**, 1.

Nowell, P. C. (1976). The clonal evolution of tumor cell populations. *Science* **194**, 23.

Oh, I. H. and Reddy, E. P. (1999). The myb gene family in cell growth, differentiation and apoptosis. *Oncogene* **18**, 3017.

Peters, C. W., Sippel, A. E., Vingron, M. and Klempnauer, K. H. (1987). Drosophila and vertebrate myb proteins share two conserved regions, one of which functions as a DNA-binding domain. *EMBO J.* **6**, 3085.

Pihan, G. A., Purohit, A., Wallace, J., Knecht, H., Woda, B., Quesenberry, P. and Doxsey, S. J. (1998). Centrosome defects and genetic instability in malignant tumors. *Cancer Res.* **58**, 3974.

Poodry, C. (1980). Generation of a *shi*$^{+}$ chromosome. *Drosophila Information Service* **55**, 210.

Poodry, C. A. (1975). Autonomous and non-autonomous cell death in the metamorphosis of the epidermis of *Drosophila*. *Wilhelm Roux Arch.* **178**, 333.

Reed, J. C. (1999). Mechanisms of apoptosis avoidance in cancer. *Curr. Opin. Oncol.* **11**, 68.

Salisbury, J. L., Whitehead, C. M., Lingle, W. L. and Barrett, S. L. (1999). Centrosomes and cancer. *Biol. Cell* **91**, 451.

Shermoen, A. W. (2000). BrdU labeling of chromosomes. In Drosophila *Protocols* (ed. W. Sullivan, M. Ashburner and R. S. Hawley), pp. 57. New York: Cold Spring Harbor Laboratory Press.

Sluder, G. and Hinchcliffe, E. H. (1999). Control of centrosome reproduction: the right number at the right time. *Biol. Cell* **91**, 413.

Solomon, E., Borrow, J. and Goddard, A. D. (1991). Chromosome aberrations and cancer. *Science* **254**, 1153.

Stern, B., Ried, G., Clegg, N. J., Grigliatti, T. A. and Lehner, C. F. (1993). Genetic analysis of the Drosophila cdc2 homolog. *Development* **117**, 219.

Su, T. T., Sprenger, F., DiGregorio, P. J., Campbell, S. D. and O'Farrell, P. H. (1998). Exit from mitosis in Drosophila syncytial embryos requires proteolysis and cyclin degradation, and is associated with localized dephosphorylation. *Genes Dev.* **12**, 1495.

Taylor, D., Badiani, P. and Weston, K. (1996). A dominant interfering Myb mutant causes apoptosis in T cells. *Genes Dev.* **10**, 2732.

Theurkauf, W. E. (1994). Immunofluorescence analysis of the cytoskeleton during oogenesis and early embryogenesis. *Methods Cell Biol.* **44**, 489.

Tutt, A., Gabriel, A., Bertwistle, D., Connor, F., Paterson, H., Peacock, J., Ross, G. and Ashworth, A. (1999). Absence of Brca2 causes genome instability by chromosome breakage and loss associated with centrosome amplification. *Curr. Biol.* **9**, 1107.

Vidwans, S. J., Wong, M. L. and O'Farrell, P. H. (1999). Mitotic regulators govern progress through steps in the centrosome duplication cycle. *J. Cell Biol.* **147**, 1371.

Weston, K. (1998). Myb proteins in life, death and differentiation. *Curr. Opin. Genet. Dev.* **8**, 76.

Whitfield, W. G., Millar, S. E., Saumweber, H., Frasch, M. and Glover, D. M. (1988). Cloning of a gene encoding an antigen associated with the centrosome in Drosophila. *J. Cell Sci.* **89**, 467.

Xu, X., Weaver, Z., Linke, S. P., Li, C., Gotay, J., Wang, X. W., Harris, C. C., Ried, T. and Deng, C. X. (1999). Centrosome amplification and a defective G2-M cell cycle checkpoint induce genetic instability in BRCA1 exon 11 isoform-deficient cells. *Mol. Cell* **3**, 389.